Published in final edited form as:

Nat Struct Mol Biol. 2008 November ; 15(11): 1169–1175. doi:10.1038/nsmb.1499.

The H3K36 demethylase Jhdm1b/Kdm2b regulates cell proliferation and senescence through p15^{Ink4b}

Jin He[1,2,3], **Eric M. Kallin**[1,2,3], **Yu-ichi Tsukada**[1,2], and **Yi Zhang**[1,2,*]

[1]Howard Hughes Medical Institute, Lineberger Comprehensive Cancer Center, University of North Carolina at Chapel Hill, Chapel Hill, North Carolina 27599-7295

[2]Department of Biochemistry and Biophysics, Lineberger Comprehensive Cancer Center, University of North Carolina at Chapel Hill, Chapel Hill, North Carolina 27599-7295

Abstract

The *Ink4a/Arf/Ink4b* locus plays a critical role in both cellular senescence and tumorigenesis. Jhdm1b/Kdm2b/Fbxl10, the mammalian paralogue of the histone demethylase Jhdm1a/Kdm2a/Fbxl11, has been implicated in cell cycle regulation and tumorigenesis. In this report, we demonstrate that Jhdm1b is an H3K36 demethylase. Knockdown of *Jhdm1b* in primary MEFs inhibits cell proliferation and induces cellular senescence in a pRb and p53 pathway-dependent manner. Importantly, the effect of Jhdm1b on cell proliferation and cellular senescence is mediated through de-repression of *p15^{Ink4b}* as loss of p15^{Ink4b} function rescues cell proliferation defects in Jhdm1b knockdown cells. Chromatin immunoprecipitation on ectopically expressed Jhdm1b demonstrates that Jhdm1b targets the *p15^{Ink4b}* locus and regulates its expression in an enzymatic activity-dependent manner. Alteration of Jhdm1b level affects Ras-induced neoplastic transformation. Collectively, our results indicate that Jhdm1b is an H3K36 demethylase that regulates cell proliferation and senescence through p15^{Ink4b}.

Introduction

The *Ink4a/Arf/Ink4b* locus encodes three critical cell cycle inhibitors including p16^{Ink4a}, p15^{Ink4b} and Arf (p14 in human and p19 in mouse). The two members of the Ink4 protein family inhibit the binding of D-type cyclins to cyclin dependent kinase 4 and 6 (Cdk4/6), inhibiting the phosphorylation of retinoblastoma (Rb) family proteins and preventing G1/S phase transition in cells. The Arf protein, which shares two common *p16^{Ink4a}* exons but contains a distinct open reading frame, is able to activate the p53 pathway through sequestration of the p53 negative regulator Mdm2 (reviewed in1,2).

The *Ink4a/Arf/Ink4b* locus plays a critical role in determining cellular response to oncogenic signals. In normal cells, inappropriate oncogenic stimulation activates this locus and leads to cellular senescence. However, dysregulation of this locus can facilitate tumorigenesis

*To whom correspondence should be addressed, Phone: 919-843-8225, Fax: 919-966-4330, e-mail: yi_zhang@med.unc.edu.
[3]These authors contributed to this work equally

through multiple oncogenic signaling pathways. The importance of this locus in cellular defense against tumorigenesis is further supported by evidence that *Ink4a/Arf/Ink4b* is frequently deleted or mutated in a variety of human primary tumors3–6. In addition, combined deletion of *Ink4a/Arf* with *Ink4b* in mice results in a broader spectrum of tumors compared to mice with individual genetic deletions indicating that genes in this locus work synergistically to prevent tumor development and that $p15^{Ink4b}$ is a critical tumor suppressor in the absence of $p16^{Ink4a}$ 7. Since this locus controls both cellular senescence and tumorigenesis, tight regulation is crucial under physiological conditions. Although many oncoproteins and Polycomb group proteins have been shown to regulate *Ink4a/Arf* expression8,9, the mechanism that controls $p15^{Ink4b}$ expression remains unclear.

The JmjC-domain containing histone demethylase 1b (Jhdm1b) is a paralogue of the first identified histone lysine demethylase, Jhdm1a, which targets H3K36 for demethylation10. This fact, as well as their high homology within the catalytic JmjC domain (79%), led us to predict that the demethylase activity against the H3K36 methyl group is conserved between both paralogues (Supplementary Fig. 1). However, in a recent report Jhdm1b was implicated in the demethylation of H3K4me3 *in vivo*11. In addition, the reported biological functions of this protein are also controversial. Although two groups have identified *Jhdm1b* as a hotspot for proviral insertion in murine tumors generated by random MMLV mutagenesis, the locus has paradoxically been identified as an oncogene and a tumor suppressor depending on the screen and functional studies used12,13. In addition, subsequent studies have reported that Jhdm1b was a negative regulator of *c-Jun*14 or rRNA genes11, further implicating Jhdm1b in tumor suppression.

In an effort to resolve these apparent discrepancies, we set out to use methods well established in our previous studies to characterize the biochemical properties as well as biological function of Jhdm1b using primary MEF cells, which maintain normal cell cycle regulatory pathways, to study protein function. We report here that Jhdm1b is an H3K36-specific histone demethylase that functions to promote cellular proliferation and inhibit cellular senescence through the silencing of the $p15^{Ink4b}$ tumor suppressor gene.

Results

Jhdm1b is an H3K36me2-specific demethylase

In an effort to explain the difference between activity prediction based on domain homology and reported *in vivo* substrate specificity11, we first investigated the *in vitro* and *in vivo* catalytic activity of Jhdm1b. To this end, recombinant protein was flag-affinity purified from baculovirus-infected Sf9 cells (Supplementary Fig. 2a), and subjected to an histone demethylase assay by measuring radioactive formaldehyde release10. Results shown in Figure 1a demonstrate that, of all the substrates tested, only the H3K36-specific SET2 labeled histone substrate can be demethylated by Jhdm1b, indicating that as predicted Jhdm1b has a similar substrate specificity to JHDM1A10.

Since the protein was implicated in the demethylation of H3K4me3 *in vivo*11, we tested the capacity of Jhdm1b to demethylate H3K4me3 *in vitro*. To this end, we purified a new batch of wild-type Jhdm1b along with a mutant Jhdm1b (H211A) predicted to kill the enzymatic

activity (Supplementary Fig. 2b). As controls, we also purified the H3K36me2-specific demethylase, JHDM1A10, and the H3K4me3-specific demethylase, RBP215. Incubation of these proteins with SET2-labeled histone substrate confirmed efficient formaldehyde release for JHDM1A and Jhdm1b, but not Jhdm1b (H211A) (Fig. 1b). In addition, Jhdm1b exhibited about one third the activity of JHDM1A when equivalent amount of proteins were assayed. Furthermore, incubation of these proteins with substrate labeled by a mutated form of the SET7, SET7 (Y245A), which generates K4me2 and K4me316, did not show efficient release of formaldehyde above background. However, incubation of RBP2 with the same substrate resulted in formaldehyde release (Fig. 1b), demonstrating that Jhdm1b has no H3K4me3 demethylase activity under the assay conditions.

To further define the substrate specificity of Jhdm1b, we incubated the protein with core histones purified from HeLa cells and analyzed the product by Western blot using methylation state-specific antibodies. These experiments demonstrate that Jhdm1b, like its paralogue, JHDM1A, can specifically demethylate H3K36me2 and H3K36me1 histone substrates (Fig. 1c). However, it does not alter H3K4 methylation levels (Fig. 1c).

To characterize the substrate specificity of Jhdm1b *in vivo*, we utilized HEK293 cells selected for adherence (AD293) and overexpressed Jhdm1b and Jhdm1b (H211A) via retroviral infection. Quantitative reverse transcriptase PCR (qRT-PCR) verified similar levels of stable expression of wild-type and the mutant Jhdm1b (Fig. 1d). Western blot analysis demonstrated that overexpression of wild-type, but not the mutant, Jhdm1b resulted in marked decrease of H3K36me2 levels (Fig. 1e). Although a small decrease in H3K36me3, as well as H3K4me3 was observed, the minor decrease did not rely on a functional JmjC domain as it can also be seen in the cells over expressing the catalytic mutant. Given that overexpression of Jhdm1b in HeLa cells was previously reported to result in the decrease of H3K4me3 levels11, we overexpressed Jhdm1b in HeLa cells by lentiviral infection. Western blot analysis of the histones purified from the infected HeLa cells confirmed our observation in the HEK293 cells (Supplementary Fig. 3a). Taken together, our results indicate that Jhdm1b is an H3K36 rather than H3K4-specific demethylase.

Jhdm1b knockdown inhibits cell proliferation and induces senescence

We next explored the function of Jhdm1b in primary cells. Given that previous analyses of Jhdm1b tumor suppressor function had been carried out in transformed or immortalized cell lines, we postulated that the paradoxical conclusions regarding the role of Jhdm1b in cancer might be due to the many genetic alterations necessary for the establishment of these cell lines. We therefore designed an shRNA that can target all three murine isoforms of *Jhdm1b* and introduced it into primary mouse embryonic fibroblast (MEF) cells by lentiviral infection (Jhdm1b KD). After selection, the knockdown efficiency (90%) was verified by qRT-PCR (Fig. 2a). Interestingly, stable knockdown of Jhdm1b resulted in a substantial decrease in cell proliferation (Fig. 2b), a phenotype reminiscent of that displayed by MEF cells with reduced levels of the Polycomb group protein Ring1b20,21. Based on this observation, shRNA directed against *Ring1b* was introduced into MEF cells (Ring1b KD), and knockdown efficiency was determined to be 90% by qRT-PCR (Fig. 2a). Furthermore,

knockdown of *Jhdm1b* had no substantial effect on *Ring1b* levels and vice versa (Fig. 2a). Comparison of the cell proliferation levels of *Ring1b* KD, *Jhdm1b* KD, and control cells confirmed Ring1b's drastic effects on cell proliferation and indicated that *Jhdm1b* knockdown, while drastic, did not achieve the same level of cell growth inhibition as that of *Ring1b* knockdown (Fig. 2b). BrdU pulse labeling followed by flow cytometry analysis revealed that *Jhdm1b* KD resulted in a 2-fold reduction in the number of cells in S-phase as compared to control MEFs, while a 4-fold reduction is observed in the *Ring1b* KD cells (Fig. 2c). In addition, Ring1b has been demonstrated to play an important role in regulating cellular senescence as a component of the Polycomb repressive complex 1 (PRC1) which enacts negative regulation of the $p16^{Ink4a}$ locus20,22. To investigate whether *Jhdm1b* KD also contributes to pre-mature cellular senescence, *Ring1b* and *Jhdm1b* KD MEFs were analyzed for the presence of senescence-associated β-galactosidase (SA-β-galactosidase) at different passages. While only very few cells stained positive for SA-β-galactosidase in control MEFs at passage 5, *Jhdm1b* KD MEFs underwent cellular senescence at a markedly increased rate (Fig. 2d) while *Ring1b* knockdown had the most drastic ability to induce senescence. Taken together, these results suggest that Jhdm1b is involved in the positive regulation of cell cycle and negative regulation of passage-dependant cellular senescence.

Jhdm1b regulates cell proliferation through $p15^{Ink4b}$

Cellular proliferation and senescence is tightly regulated through the p53 and pRb pathways, and both of these cellular pathways can be inhibited by the introduction of SV40 T antigen into primary cells23. To determine whether the function of Jhdm1b in cell proliferation and senescence is pRb and p53 dependent, we inactivated both pathways by retroviral expression of SV40 large T antigen in MEFs and then subjected the cells to *Jhdm1b* knockdown. Results shown in Supplementary Figure 4a demonstrate that knockdown of *Jhdm1b* does not alter the cellular proliferation of MEF cells when the p53 and pRb pathways are blocked by the SV40 large T antigen (Supplementary Fig. 4a). Consistent with this result, the percentage of S-phase cells, as indicated by BrdU incorporation, is not altered by *Jhdm1b* knockdown under these conditions (Supplementary Fig. 4b). In addition, *Jhdm1b* knockdown induced cellular senescence, as assessed by the appearance of SA-β-galactosidase staining, was also blocked in SV40 large T antigen transduced cells (Supplementary Fig. 4c). Collectively, these data suggest that Jhdm1b's pro-growth and anti-senescence properties act upstream of these two pathways.

Previous studies have identified a number of genes whose expression is linked to Rb regulated cellular senescence and p53-dependant apoptosis24. These genes include members of the *Ink4a/Arf/Ink4b* tumor suppressor locus, *p18* (also known as *Ink4c*), and the cell cycle regulators *p27* (also known as *Cdkn1b*) and *p21*. To determine whether loss of Jhdm1b function affected expression of any of these genes, we performed qRT-PCR in control, *Jhdm1b* KD, and *Ring1b* KD cells. Results shown in Fig. 3a demonstrate that *Jhdm1b* KD resulted in a marked upregulation of $p15^{Ink4b}$. In agreement with the crucial role of Ring1b in the PRC1 complex, *Ring1b* KD resulted in a substantial upregulation of $p16^{Ink4a}$ 20,22. In addition, we also observed a marked increase in $p15^{Ink4b}$ mRNA levels. The effect of *Jhdm1b* and *Ring1b* KD on $p15^{Ink4b}$ and $p16^{Ink4a}$ levels was also confirmed by Western blot (Fig. 3b). These data are consistent with the observation that the $p16^{Ink4a}$ protein has a more

potent inhibitory effect on cell proliferation, as well as the notion that $p15^{Ink4b}$ functions to back-up the function of $p16^{Ink4a}$ 7. Importantly, similar to Ring1b KD, the expression of *p21*, a p53 pathway target gene, was not altered by Jhdm1b KD (Fig. 3a). To analyze whether $p15^{Ink4b}$ is a key mediator of Jhdm1b's function in cellular proliferation, we derived primary MEFs from $p15^{Ink4b}$ null mice25 and performed knockdown of *Jhdm1b* or *Ring1b*. Results shown in Figure 3c and 3d demonstrate that loss of $p15^{Ink4b}$ function could largely rescue the slow proliferation and low BrdU incorporation caused by *Jhdm1b* knockdown. Thus, we conclude that Jhdm1b regulates cellular proliferation and senescence by negatively regulating the expression of the $p15^{Ink4b}$ tumor suppressor gene in primary cells.

Jhdm1b regulates $p15^{Ink4b}$ expression through H3K36 demethylation

H3K36 methylation, which has been linked to active gene transcription in organisms from yeast to humans, is present within the coding regions of genes being actively transcribed, and tends to peak towards the 3' end of transcribed regions25–28. The mechanism by which high levels of H3K36me2 are excluded from the promoter of active genes, as well as the functional significance of this observation is still not clear in higher eukaryotes. However, it has been demonstrated that SET2 association with elongating RNAPII is at least partly responsible for this phenomenon in yeast27. To investigate whether the demethylase activity of Jhdm1b directly contributes to $p15^{Ink4b}$ regulation and cellular proliferation, we attempted to rescue the *Jhdm1b* KD MEFs with siRNA resistant wild-type F-Jhdm1b as well as catalytically deficient mutant, F-Jhdm1b (H211A). After confirming equal expression of the rescue constructs (Supplementary Fig. 5), we analyzed their effects on cellular proliferation. Results shown in Figure 4a demonstrate that re-introduction of wild-type Jhdm1b rescued the growth defects, while re-introduction of the catalytic-defective mutant did not. In addition, re-introduction of wild-type Jhdm1b, but not the catalytic mutant, restored $p15^{Ink4b}$ expression to control levels (Fig. 4b). Thus, both normal cell proliferation and $p15^{Ink4b}$ repression depends on the demethylase activity of Jhdm1b.

Having established that transcriptional repression of $p15^{Ink4b}$ depends on the H3K36-demethylase activity of Jhdm1b, we used ChIP assays to decipher whether $p15^{Ink4b}$ is a direct target of Jhdm1b. Because none of the available Jhdm1b antibodies worked in immunoprecipitation in our hands, we resolved to retrovirally express F-Jhdm1b in primary MEF cells and performed ChIP assays using Flag antibodies. F-Jhdm1b was found to be specifically enriched 3-fold above background in regions just upstream (amplicon 1) and surrounding the transcription start site (amplicon 2) of $p15^{Ink4b}$ when compared with mock infected cells (Fig. 4c, d). However, the protein was not enriched within the $p15^{Ink4b}$ intron (amplicon 3) (Fig. 4c, d). ChIP analysis of H3K36me2 levels at these same regions in *Jhdm1b* KD and control cells revealed that KD of *Jhdm1b* resulted in an increase in the H3K36me2 levels across the locus when compared to control cells (Fig. 4e), suggesting that Jhdm1b might also play an active role in the demethylation of H3K36me2 downstream of the transcription start site. However, it has not escaped our attention that increased transcription of the gene may itself contribute to increases in H3K36me2 within the coding region. Furthermore, rescue of the KD by wild-type Jhdm1b resulted in H3K36me2 levels below those of control cells (Fig. 4e). In addition, H3K36me2 levels within the *Gapdh* locus were unchanged for all samples (data not shown). Taken together, these data suggest that

p15^{Ink4b} is a direct Jhdm1b target and that Jhdm1b regulates *p15*^{Ink4b} expression through active demethylation of H3K36.

Jhdm1b cooperates with Ras to induce oncogenic transformation

All of the data presented above indicates that Jhdm1b functions as a proto-oncogene through its ability to repress transcription of the *p15*^{Ink4b} locus. In an effort to further establish the oncogenic potential of Jhdm1b, we assessed the contribution of the protein to colony formation using knockdown or overexpression in *p53* null MEFs followed by superinfection of retroviral H-Ras12V virus. Results of soft-agar colony formation analysis indicate that co-expression of RAS and Jhdm1b in *p53* null MEF cells results in an increase in Ras induced oncogenic transformation (Fig. 5a). Conversely, knockdown of *Jhdm1b* inhibited Ras-induced colony formation (Fig. 5b). Together these data support the notion that *Jhdm1b* acts as a proto-oncogene in primary fibroblast cells.

Discussion

In this report, we demonstrate that Jhdm1b, like its paralogue Jhdm1a, functions as an H3K36 demethylase *in vitro* and *in vivo*. Recombinant Jhdm1b purified from baculovirus infected Sf9 cells demethylates H3K36me2 *in vitro* in a radioactive formaldehyde release assay and in histone Western blot analysis (Fig. 1) and Western blotting and ChIP analysis indicate that overexpression of Jhdm1b results in global H3K36me2 demethylation (Fig. 1e), as well as gene-specific H3K36me2 demethylation (Fig. 4) in different cell types including HeLa and HEK293 cells (Supplementary Fig. 3a). In addition, the previously suggested nucleolar staining pattern of Jhdm1b could not be observed in either HeLa cells11 (Supplementary Fig. 3b), or AD293 cells (Supplementary Fig. 5b).

In addition to the substrate specificity of Jhdm1b, its role in tumorigenesis has also been a point of contention. One of the earliest reports of Jhdm1b function came out of a genetic screen for tumor suppressor genes in mouse lymphomas13. The authors identified several bi-allelic retroviral insertion events at the *Jhdm1b* locus when several of the induced lymphomas were analyzed. However, further analysis of additional tumor samples revealed locus insertion that left the *Jhdm1b* coding region intact. This leaves open the possibility that the tumor manifesting retroviral insertions could either activate or suppresses *Jhdm1b* function. Therefore, the potential of *Jhdm1b* to serve as an oncogene or tumor suppressor was not resolved in this study. In addition some indirect evidence suggested Jhdm1b may act as a tumor suppressor, including a link to the negative regulation of *c-Jun*14, as well as a description of its role in the negative regulation of rRNA genes11. However, these experiments were carried out in various cell lines in which critical pathways important for cellular senescence and tumorigenesis (such as *Ink4a/Arf/Ink4b*) are also disrupted. Thus further evidence would be required to support the relevance of previously identified gene targets in a normal context. Arecent report that screened 44 random MMLV induced T cell lymphomas identified the *Jhdm1b* locus as an insertion hotspot12. This study revealed multiple, orientated provirus insertions upstream of the canonical *Jhdm1b* promoter and further implicated a role for Jhdm1b overexpression in the immortalization of primary MEF cells. In this study, we provide several lines of evidence that support *Jhdm1b* may indeed be

a proto-oncogene. First, we demonstrate in primary MEFs that knockdown of Jhdm1b resulted in cell proliferation defects and increased senescence (Fig. 2). Furthermore, we demonstrate that Jhdm1b contributes to the regulation of cell proliferation and senescence by directly repressing the expression of the *p15*^{Ink4b} tumor suppressor (Fig. 3 and Fig 4). Importantly, *p15*^{Ink4b} appears to be a major target that mediates Jhdm1b function in cellular proliferation since loss of *p15*^{Ink4b} function can largely rescue the *Jhdm1b* knockdown effects (Fig. 4). Finally, Jhdm1b can cooperate with Ras to transform primary MEF cells (Fig. 5). Therefore, we conclude that Jhdm1b is indeed a proto-oncogene which functions at least partially by controlling the expression of the *p15*^{Ink4b} tumor suppressor through removal of H3K36me2.

Methods

Cloning, cell line generation

All of the cell lines used in this study were maintained in Dulbeccos's modified Eagle's medium supplemented with 10% (v/v) fetal bovine serum and 1% (v/v) penicillin/streptomycin. Primary MEFs harvested from day 13.5 C57BL/6 and *p15*^{Ink4b} null mouse embryos were plated into a P75 flask. The confluent cells were frozen down and considered passage 1. The cells were split at 1:5 for each passage. Cell growth was measured by plating 5×10^5 MEFs on a 100mm plate in triplicate for each group. The cell number was counted using a hemocytometer at the time points indicated. Selection and stable maintenance of exogenous plasmids was accomplished in the presence of either 1μg ml^{-1} (AD293 cells) or 4μg ml^{-1} (MEF cells) puromycin. PCR amplification of an EST clone corresponding to full length Jhdm1B (NM_001003953) was cloned into a modified pFastBacHT B vector (Invitrogen) containing an N terminal flag epitope tag for baculovirus generation as per manufacturer's protocol (Invitrogen). Full length Jhdm1B was subcloned into pMSCVpuro vector (Clontech) for stable cell line generation using the manufacturer's protocol. Jhdm1b (H211A) mutant was generated by employing overlapping PCR/subcloning. Stable knockdown was achieved using a lentiviral system obtained from the NIH AIDS Research and Reference Reagent Program. The mouse U6 promoter was cloned from mouse genomic DNA and inserted into the NotI site of pTY-EF1a-nLacZ. For the LV-U6 shRNA-Pgk-Pac construct, the Pgk-Pac cassette at NotI/EcoRI sites replaced the EF1a-nLacZ cassette. The hairpin RNA targeting Jhdm1b (5'-GCTCCAACTCAGTTACTGT-3'), Ring1b (5'-GCAGTACACCATTTACATA-3') and control (5'-GTTCAGATGTGCGGCGAGT-3') were cloned into BBSI/HindIII sties under the U6 promoter 29. To generate wild type and mutant Jhdm1b (H211A) rescue constructs, the siRNA target site of Jhdm1b was mutated to ATTGCAGTTGAGTTACTGT by PCR mutagenesis. The siRNA resistant wild type and mutant Jhdm1b cDNAs were PCR amplified and cloned into either SpeI/EcoRI site of LV vector or NotI/XbaI of RV vector.

In vitro histone demethylase formaldehyde release assay

Histone substrates were radiolabeled and formaldehyde release assays were performed as previously described10,30. Unless otherwise stated, 5μg of Flag purified recombinant protein was incubated in the presence of labeled substrate corresponding to 60,000 input counts and demethylase buffer (50 mM HEPES-KOH (pH 8.0), 70 mM $Fe(NH4)_2(SO4)_2$, 1

mM α-ketoglutarate, 2 mM ascorbate) for one hour at 37°C. Released, labeled formaldehyde was extracted using a modified NASH technique and subjected to scintillation counting. Data is presented as counts per minute in the extracted sample.

Western blot analysis and immunostaining

Total protein was extracted by RIPA buffer. Purified native histones from HeLa cells or acid extracted histones from the indicated cell lines were prepared as previously described31. Antibodies against specific methylation states were used at dilutions ranging from 1:250 – 1:1000: H3K36me1(Abcam 9048), H3K36me210 H3K36me3(Abcam 9050), H3K4me1(Abcam 8895), H3K4me2 (Abcam 7766), H3K4me3(Abcam 8580). Blots were normalized using an antibody against pan H3 (Abcam 1791). Anti-p21(Santa Cruz SC-397), anti-$p15^{Ink4b}$ (Cell Signaling 4822), and anti-$p16^{Ink4a}$ (Santa Cruz SC-1207) were used at dilution of 1:1000 for Western Blot. Indirect immunostaining was carried out using primary MEFs and Hela cells. The cells were plated onto cover slips in 6 well plates after LV transduction, fixed 48 hours post transduction for 20 min in 4% (w/v) paraformaldehyde, washed with three times with PBS, and subsequently permeabilized for 20 min in 0.5% (v/v) Triton-X-100/PBS. Permeablized cells were blocked in 3% (w/v) BSA/PBS for 30min and incubated with Flag monoclonal M2 antibody (Sigma) at 1:1000 dilution in a humidified chamber for 3 hours. After incubation, cells were washed 3 times and incubated with FITC or Rhodamine conjugated secondary antibodies (Jackson ImmunoResearch Laboratories) at dilution of 1:500. Cells were washed twice with PBS, stained with 4,6-diamidino-2-phenylindole dihydrochloride (DAPI), and mounted on glass slides in fluorescence mounting medium (DAKO). Slides were analyzed on an Axiovert 200 fluorescent microscope (Zeiss).

BrdU incorporation and cycle cycle analysis

MEFs were grown in the presence of 10 μM BrdU for 60min. The cells were harvested and fixed overnight using 75% ethanol. Fixed cells were stained with FITC conjugated mouse anti-BrdU antibody (BD biosciences, 347583) and propidium iodide. The stained cells were analyzed by flow cytometry (BD FACSCalibur) and data was analyzed using WinMDI version 2.9 (TSRI flowcytometry Software).

Senescence associated-β-galactosidase assay

Cells were washed twice with PBS and immersed in fixation buffer (2% (w/v) formaldehyde, 0.2% (w/v) glutaraldehyde in PBS) for 10 min. After two additional PBS washes the cells were allowed to stain overnight in staining solution (40 mM citric acid/ sodium phosphate pH 6.0, 150 mM NaCl, 2.0 mM $MgCl_2$, 1 mg ml^{-1} x-gal).

Reverse transcription / qPCR

RNA was extracted and purified from cell lines using Qiashredder (Qiagen) and RNeasy (Qiagen) spin columns; DNase treated (Promega RQ1 Dnase) and cleaned up using Qiagen RNeasy column (Qiagen). 1μg of RNA was subjected to reverse transcription using random primers (Promega) and Improm-II reverse transcription kit (Promega). cDNA levels were assayed via Real time PCR using SYBR GreenER (Invitrogen) and analyzed on an ABI

7300 Real Time PCR System with SDS software version 1.3.1. qRT-PCR primer sequences are available in Supplementary Table 1.

ChIP assay

ChIP assays employing flag-antibody were carried out as previously reported32 with the following modifications: 20μl of M2 agarose (Sigma) was used in the immunoprecipitation and chromatin-bound beads were washed three times each in TSEI (0.1% [w/v] SDS, 1% [v/v] Triton-X-100, 2 mM EDTA, 150 mM NaCl, 20 mM Tris [pH 8.1]) TSEII (0.1% [w/v] SDS, 1% [v/v] Triton-X-100, 2mM EDTA, 500 mM NaCl, 20 mM Tris [pH 8.1]) and TSEIII (0.25M LiCl, 1% [v/v] NP-40, 1% [w/v] deoxycholate, 1mM EDTA, 10mM Tris [pH 8.1]) followed by two washes in TE. Histone modification ChIPs were carried out as previously reported33. ChIP DNA was analyzed via qPCR and data are presented as percentage of input as determined using Applied Biosystems's SDS software Absolute Quantification protocol. Primer sequences are available in Supplementary Table 1.

Soft agar colony assay

p53 null MEFs were transduced with different LVs. 48 hours after transduction, the cells were superinfected with retroviral H-Ras12V virus. 5000 cells were mixed in the 0.35% (w/v) top agar and plated onto 0.5% (w/v) basal agar. 14 days after plating, the cells were stained with 0.005% (w/v) crystal violet and colony number was counted.

Standard error reporting

All *in vitro* formaldehyde release assays and cell based assays were performed in triplicate and error bars represent the standard deviation of three independent experiments. ChIP assays and qRT-PCR experiments were repeated at least twice and data is reported for one of the biological replicates. Error bars represent the standard deviation of three qPCR reactions as determined by SDS 1.3.1 software (Applied Biosystems). Soft agar colony assays were performed and error bars represent the standard deviation of large colony numbers between three separate plating replicates.

Supplementary Material

Refer to Web version on PubMed Central for supplementary material.

Acknowledgments

We would like to thank Dr. Linda Wolff (National Cancer Institute) for the $p15^{Ink4b}$ null mice. This work is partially supported by NIH (GM068804). J.H. is a fellow of the Leukemia and Lymphoma Society. Y.Z. is an investigator of the Howard Hughes Medical Institute.

References

1. Gil J, Peters G. Regulation of the INK4b-ARF-INK4a tumour suppressor locus: all for one or one for all. Nat Rev Mol Cell Biol. 2006; 7:667–677. [PubMed: 16921403]
2. Ortega S, Malumbres M, Barbacid M. Cyclin D-dependent kinases, INK4 inhibitors and cancer. Biochim Biophys Acta. 2002; 1602:73–87. [PubMed: 11960696]
3. Kamb A, et al. A cell cycle regulator potentially involved in genesis of many tumor types. Science. 1994; 264:436–440. [PubMed: 8153634]

4. Kannengiesser C, et al. New founder germline mutations of CDKN2A in melanoma-prone families and multiple primary melanoma development in a patient receiving levodopa treatment. Genes Chromosomes Cancer. 2007; 46:751–760. [PubMed: 17492760]
5. Ogawa S, et al. Homozygous loss of the cyclin-dependent kinase 4-inhibitor (p16) gene in human leukemias. Blood. 1994; 84:2431–2435. [PubMed: 7919362]
6. Okuda T, et al. Frequent deletion of p16INK4a/MTS1 and p15INK4b/MTS2 in pediatric acute lymphoblastic leukemia. Blood. 1995; 85:2321–2330. [PubMed: 7727766]
7. Krimpenfort P, et al. p15Ink4b is a critical tumour suppressor in the absence of p16Ink4a. Nature. 2007; 448:943–946. [PubMed: 17713536]
8. Bracken AP, et al. The Polycomb group proteins bind throughout the INK4A-ARF locus and are disassociated in senescent cells. Genes Dev. 2007; 21:525–530. [PubMed: 17344414]
9. Kotake Y, et al. pRB family proteins are required for H3K27 trimethylation and Polycomb repression complexes binding to and silencing p16INK4alpha tumor suppressor gene. Genes Dev. 2007; 21:49–54. [PubMed: 17210787]
10. Tsukada Y, et al. Histone demethylation by a family of JmjC domain-containing proteins. Nature. 2006; 439:811–816. [PubMed: 16362057]
11. Frescas D, Guardavaccaro D, Bassermann F, Koyama-Nasu R, Pagano M. JHDM1B/FBXL10 is a nucleolar protein that represses transcription of ribosomal RNA genes. Nature. 2007; 450:309–313. [PubMed: 17994099]
12. Pfau R, et al. Members of a family of JmjC domain-containing oncoproteins immortalize embryonic fibroblasts via a JmjC domain-dependent process. Proc Natl Acad Sci U S A. 2008; 105:1907–1912. [PubMed: 18250326]
13. Suzuki T, Minehata K, Akagi K, Jenkins NA, Copeland NG. Tumor suppressor gene identification using retroviral insertional mutagenesis in Blm-deficient mice. Embo J. 2006; 25:3422–3431. [PubMed: 16858412]
14. Koyama-Nasu R, David G, Tanese N. The F-box protein Fbl10 is a novel transcriptional repressor of c-Jun. Nat Cell Biol. 2007; 9:1074–1080. [PubMed: 17704768]
15. Klose RJ, et al. The retinoblastoma binding protein RBP2 is an H3K4 demethylase. Cell. 2007; 128:889–900. [PubMed: 17320163]
16. Xiao B, et al. Structure and catalytic mechanism of the human histone methyltransferase SET7/9. Nature. 2003; 421:652–656. [PubMed: 12540855]
17. Klose RJ, et al. Demethylation of histone H3K36 and H3K9 by Rph1: a vestige of an H3K9 methylation system in Saccharomyces cerevisiae? Mol Cell Biol. 2007; 27:3951–3961. [PubMed: 17371840]
18. Yamane K, et al. PLU-1 is an H3K4 demethylase involved in transcriptional repression and breast cancer cell proliferation. Mol Cell. 2007; 25:801–812. [PubMed: 17363312]
19. Yamane K, et al. JHDM2A, a JmjC-containing H3K9 demethylase, facilitates transcription activation by androgen receptor. Cell. 2006; 125:483–495. [PubMed: 16603237]
20. Cales C, et al. Inactivation of the polycomb group protein Ring1B unveils an antiproliferative role in hematopoietic cell expansion and cooperation with tumorigenesis associated with Ink4a deletion. Mol Cell Biol. 2008; 28:1018–1028. [PubMed: 18039844]
21. Voncken JW, et al. Rnf2 (Ring1b) deficiency causes gastrulation arrest and cell cycle inhibition. Proc Natl Acad Sci U S A. 2003; 100:2468–2473. [PubMed: 12589020]
22. Jacobs JJ, Kieboom K, Marino S, DePinho RA, van Lohuizen M. The oncogene and Polycomb-group gene bmi-1 regulates cell proliferation and senescence through the ink4a locus. Nature. 1999; 397:164–168. [PubMed: 9923679]
23. Goodrich DW, Wang NP, Qian YW, Lee EY, Lee WH. The retinoblastoma gene product regulates progression through the G1 phase of the cell cycle. Cell. 1991; 67:293–302. [PubMed: 1655277]
24. Sherr CJ, Roberts JM. CDK inhibitors: positive and negative regulators of G1-phase progression. Genes Dev. 1999; 13:1501–1512. [PubMed: 10385618]
25. Bannister AJ, et al. Spatial distribution of di- and tri-methyl lysine 36 of histone H3 at active genes. J Biol Chem. 2005; 280:17732–17736. [PubMed: 15760899]

26. Martin C, Zhang Y. The diverse functions of histone lysine methylation. Nat Rev Mol Cell Biol. 2005; 6:838–849. [PubMed: 16261189]
27. Morris SA, et al. Histone H3 K36 methylation is associated with transcription elongation in Schizosaccharomyces pombe. Eukaryot Cell. 2005; 4:1446–1454. [PubMed: 16087749]
28. Rao B, Shibata Y, Strahl BD, Lieb JD. Dimethylation of histone H3 at lysine 36 demarcates regulatory and nonregulatory chromatin genome-wide. Mol Cell Biol. 2005; 25:9447–9459. [PubMed: 16227595]
29. Cao R, et al. Role of hPHF1 in H3K27 methylation and Hox gene silencing. Mol Cell Biol. 2008; 28:1862–1872. [PubMed: 18086877]
30. Zhang X, et al. Structure of the Neurospora SET domain protein DIM-5, a histone H3 lysine methyltransferase. Cell. 2002; 111:117–127. [PubMed: 12372305]
31. Wang H, et al. Role of histone H2A ubiquitination in Polycomb silencing. Nature. 2004; 431:873–878. [PubMed: 15386022]
32. Zeng PY, Vakoc CR, Chen ZC, Blobel GA, Berger SL. In vivo dual cross-linking for identification of indirect DNA-associated proteins by chromatin immunoprecipitation. Biotechniques. 2006; 41:694, 696, 698. [PubMed: 17191611]
33. Cao R, Tsukada Y, Zhang Y. Role of Bmi-1 and Ring1A in H2A ubiquitylation and Hox gene silencing. Mol Cell. 2005; 20:845–854. [PubMed: 16359901]

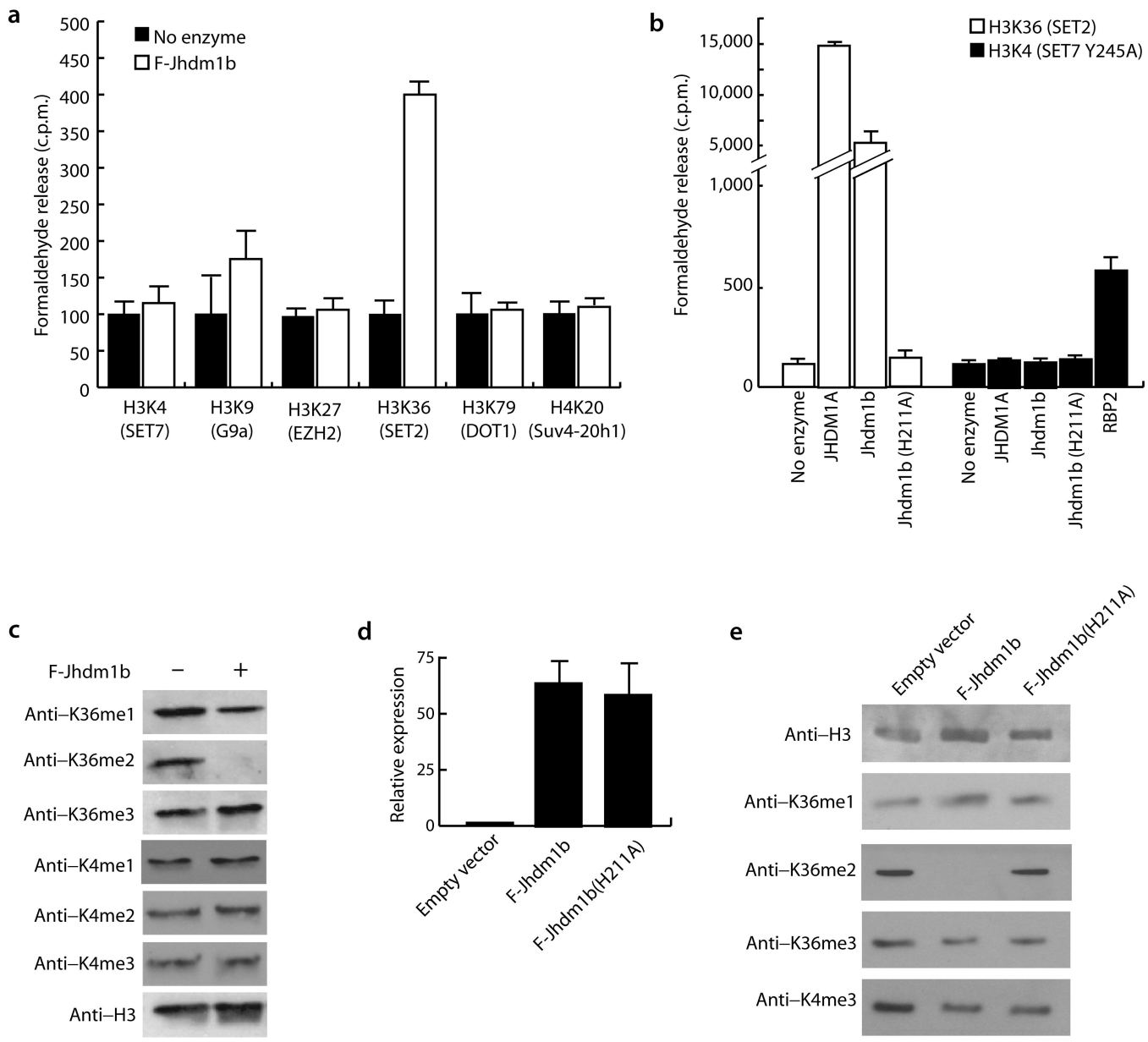

Figure 1. Jhdm1b is an H3K36-specific demethylase *in vitro* and *in vivo*

(**a**) *In vitro* formaldehyde release assay using histone substrates generated with the indicated methyltransferases and incubated with either recombinant Flag-Jhdm1b (empty bars) or no enzyme control (black bars). (**b**) *In vitro* formaldehyde release assay using recombinant Jhdm1b, Jhdm1b(H211A), JHDM1A and RBP2 incubated with H3K36-methylated (empty bars) or H3K4-methylated (black bars) substrates generated with SET2 or SET7(Y245A) methyltransferase, respectively. (**c**) HeLa cell core histones were incubated in the presence (+) or absence (−) of recombinant Jhdm1b. The resulting reaction was subjected to Western blotting with the indicated modification state-specific antibodies. (**d**) *Jhdm1b* mRNA levels from AD293 cells stably over-expressing F-Jhdm1b, F-Jhdm1b(H211A), or empty vector control cells. Samples were normalized relative to *Gapdh* and the *Jhdm1b* expression level

in the empty vector control cells was arbitrarily set to 1. (**e**) Acid extracted histones were prepared from AD293 cells stably overexpressing F-Jhdm1b or F-Jhdm1b(H211A) and subjected to Western blotting using the indicated methyl-state specific histone antibodies. All error bars represent s.d. (*n*=3).

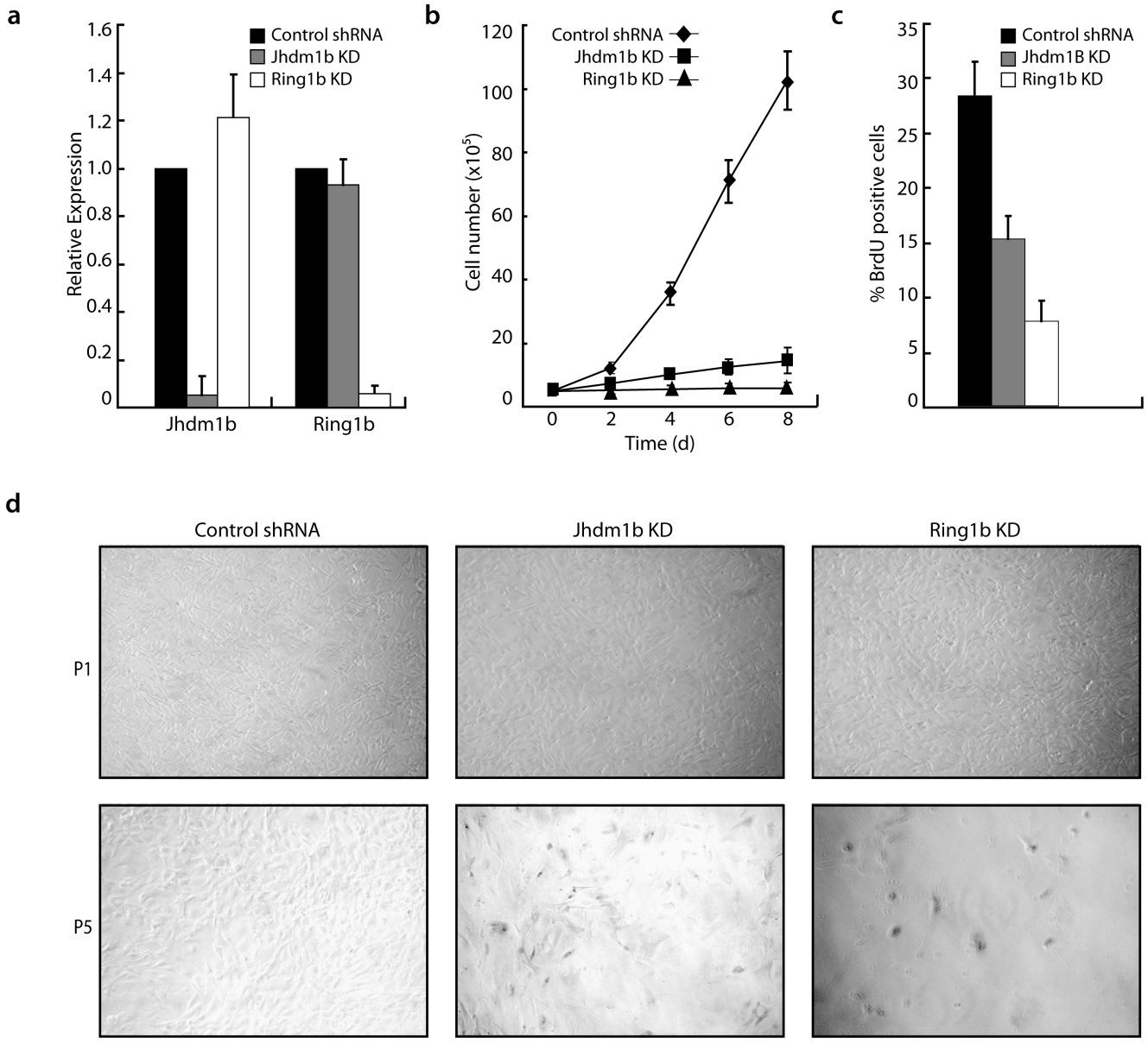

Figure 2. *Jhdm1b* knockdown in primary MEFs inhibits cell proliferation and induces cellular senescence

(**a**) Primary MEFs at passage 1 were transduced with lentiviral control (black bars), *Jhdm1b* (Jhdm1b KD, grey bars) or *Ring1b* (Ring1b KD, empty bars) shRNA and further selected by puromycin for 48 hours. mRNA levels were determined by quantitative real-time PCR (qRT-PCR). Samples were normalized against levels of *Gapdh*. The *Jhdm1b* or *Ring1b* expression level in empty vector control cells was arbitrarily set to 1. (**b**) Primary MEF cells transduced at passage 1 with lentiviral control (diamonds), *Jhdm1b* (Jhdm1b KD, squares), and *Ring1b* (Ring1b KD, triangles) shRNA and further selected by puromycin for 48 hours. 5×10^5 cells were plated and cell number was counted at different time points using a hemocytometer. (**c**) Primary MEFs were prepared as in (b), pulse labeled with BrdU and stained with PI and FITC conjugated anti-BrdU antibody. The percentage of BrdU positive

cells was determined by flow cytometry for control (black bars), Jhdm1b KD (grey bars) and Ring1b KD (empty bars). (**d**) Cells prepared as in (b) were split at 1:5 for 5 passages and senescence associated β-galactosidase activity at pH 6.0 was determined by cellular staining. Data is presented for passage 1 (P1) and passage 5 (P5) cells. All error bars represent s.d. (*n*=3).

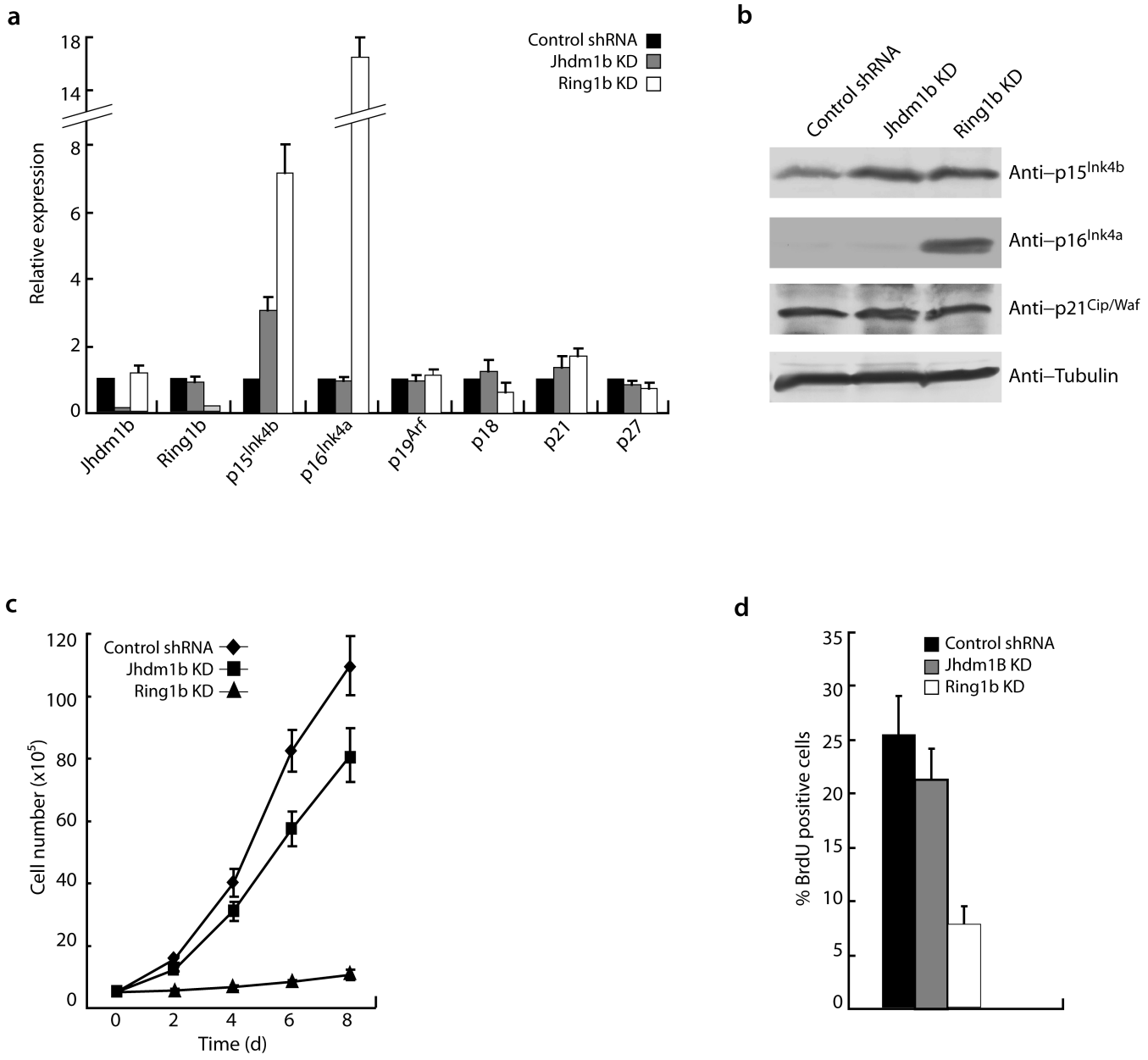

Figure 3. Jhdm1b regulates cell proliferation through p15^{Ink4b}

(**a**) Primary MEFs at passage 1 were transduced with lentiviral control (black bars), *Jhdm1b* (Jhdm1b KD, grey bars) and *Ring1b* (Ring1b KD, white bars) shRNA and further selected by puromycin for 48 hours. The expression level of the indicated genes was determined by qRT-PCR. Samples were normalized against levels of *Gapdh* and the expression level of each gene in empty vector control cells was arbitrarily set to 1. (**b**) Total protein was collected from cells prepared as in (a) and subjected to Western Blot analysis using antibodies against p15^{Ink4b}, p16^{Ink4a}, p21 and tublin. (**c**) Primary MEF cells isolated from p15^{Ink4b} null mice at passage 1 were transduced with lentiviral control (diamonds), *Jhdm1b* (Jhdm1b KD, squares), and *Ring1b* (Ring1b KD, triangles) shRNA and further selected by puromycin for 48 hours. 5×10^5 cells were plated and cell number was counted at different

time points using a hemocytometer. (**d**) Primary MEFs were prepared as in (c), pulse labeled with BrdU and stained with PI and FITC conjugated anti-BrdU antibody. The percentage of BrdU positive cells was determined by flow cytometry for control (black bars), Jhdm1b KD (grey bars) and Ring1b KD (empty bars). All error bars represent s.d. (*n*=3).

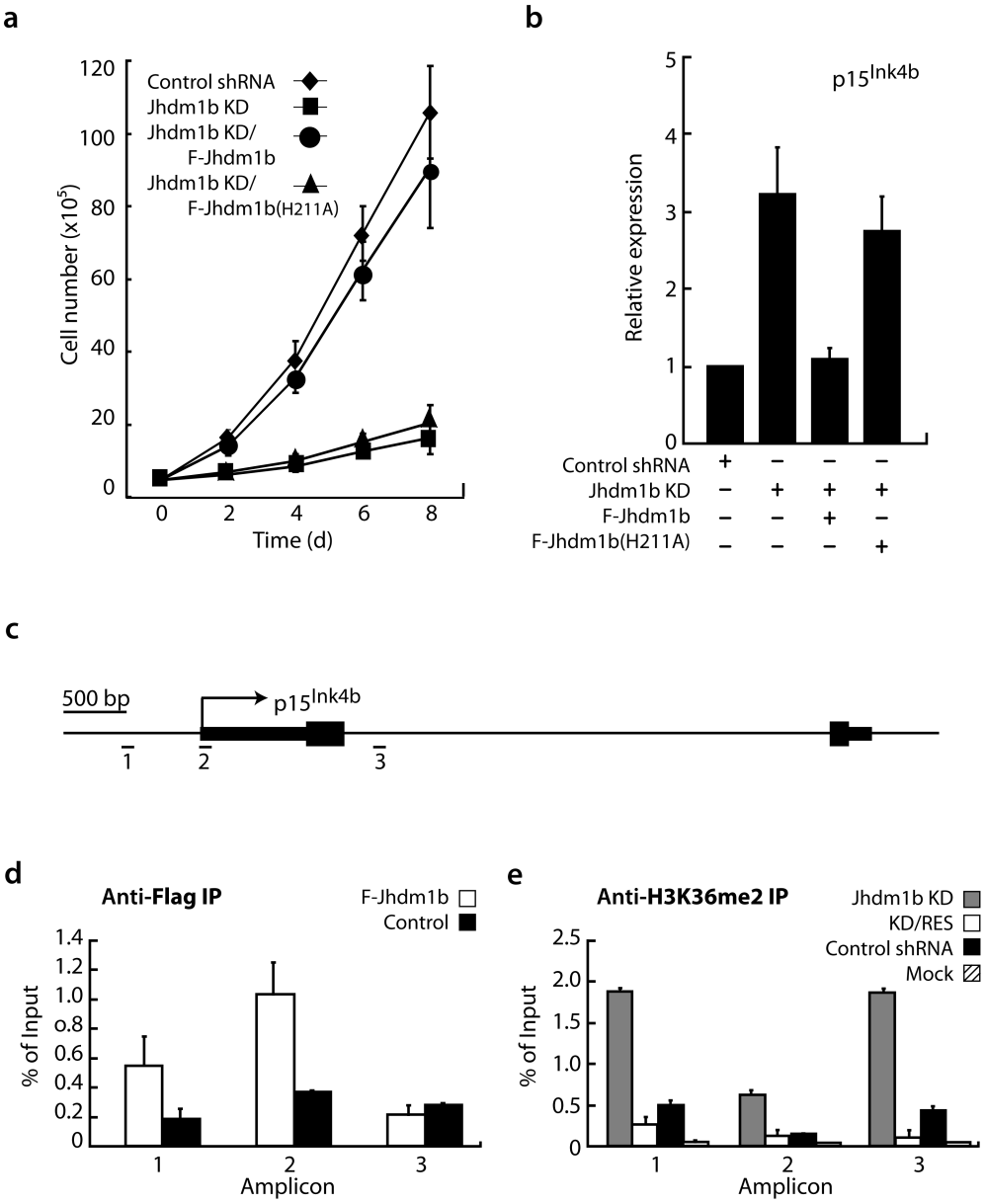

Figure 4. Jhdm1b regulates cell proliferation and *p15*^{Ink4b} expression in a histone demethylase activity-dependent manner

(**a**) Primary MEF cells were transduced with lentiviral vectors carrying control shRNA (diamonds), *Jhdm1b* shRNA (Jhdm1b KD, squares), and *Jhdm1b* shRNA with expression of F-Jhdm1b (Jhdm1b KD/F-Jhdm1b, circles) or F-Jhdm1b(H211A) (triangles). 5×10^5 cells were plated 48 hours after transduction and maintained in culture for 8 days. Cell number was counted using a hemocytometer at the indicated time points. (**b**) mRNA was collected from cells prepared as in (a) and qRT-PCR was carried out to determine *p15*^{Ink4a} expression level in each sample. Samples were normalized against levels of *Gapdh* and the expression level of each gene in empty vector control cells was arbitrarily set to 1. (**c**) Schematic representation of the *p15*^{Ink4b} locus in mouse indicating the genomic structure of the locus (exons demarcated by black boxes), as well as the location of the three amplicons studied in

ChIP experiments. (**d**) ChIP experiment utilizing chromatin prepared from primary MEF cells transduced with retrovirus encoding F-Jhdm1b (empty bars) or control virus (black bars) were carried out using antibody against Flag. F-Jhdm1b binding was assayed via qPCR at the three genomic regions depicted in (c). (**e**) ChIP experiment utilizing chromatin from primary MEFs prepared as in (a) was carried out using antibody specific for H3K36me2. H3K36me2 levels were assayed via qPCR at the three genomic regions depicted in (c). Error bars represent s.d. (n=3).

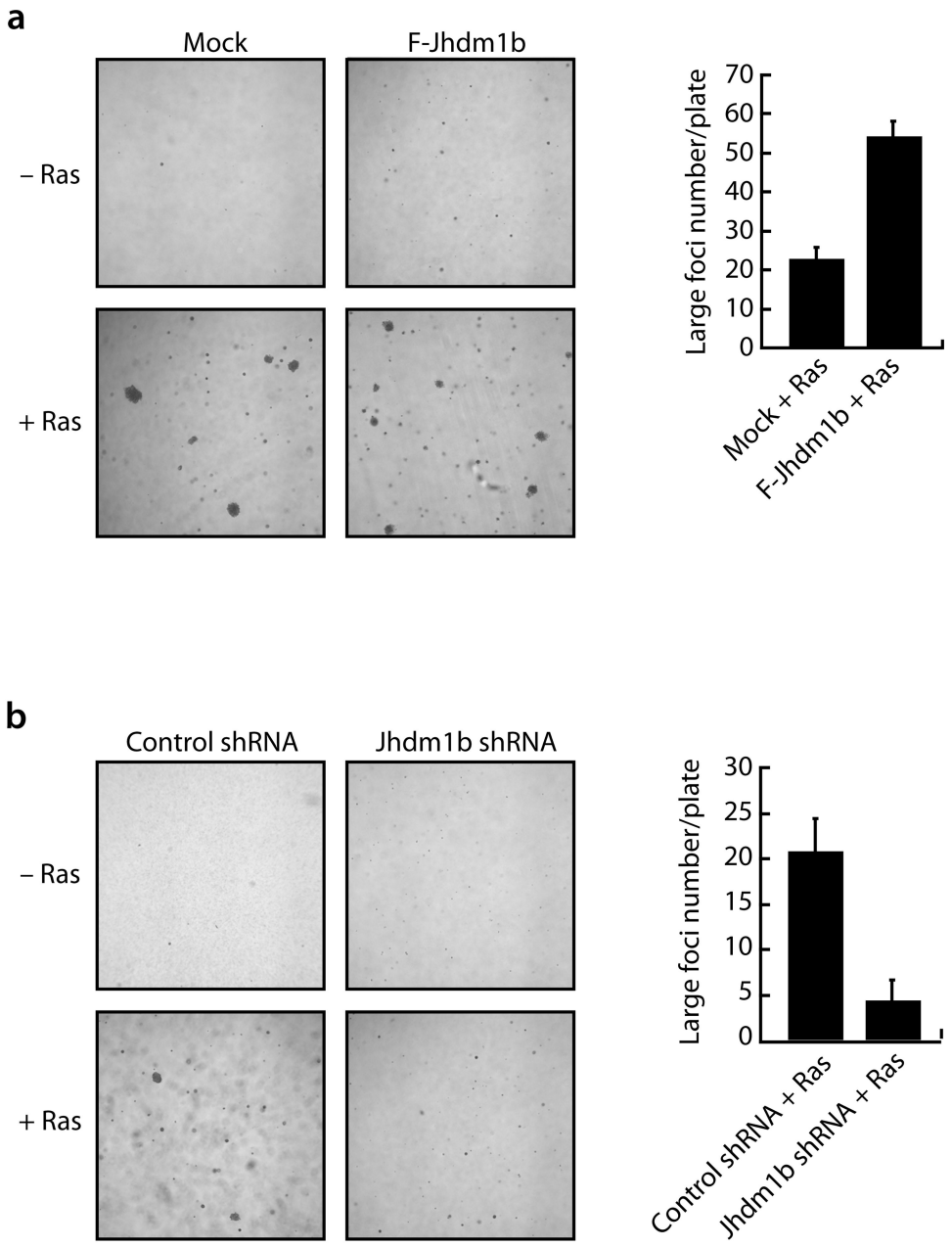

Figure 5. Jhdm1b facilitates Ras induced neoplastic transformation

(**a**) Primary MEF cells were transduced with mock or F-Jhdm1b expressing lentiviral vector followed by superinfection with retroviral H-Ras12V. 5000 cells were plated on soft agar and analyzed 14 days later. Graph represents quantification of large colonies on H-Ras transduced plates. (**b**) Primary MEF cells were transduced with lentiviral vectors carrying control shRNA (Control shRNA) or *Jhdm1b* shRNA (Jhdm1b KD) followed by puromycin selection and retroviral H-Ras12V transduction. 5000 cells were plated on soft agar and analyzed 14 days later. Graph represents quantification of large colonies on H-Ras transduced plates. All error bars represent s.d. (n=3).